A Novel Voltage Clamp Technique for Mapping Ionic Currents from Cultured Skeletal Myotubes

Blake D. Anson and William M. Roberts

Institute of Neuroscience, University of Oregon, Eugene, Oregon 97403-1254 USA

ABSTRACT   The biophysical properties and cellular distribution of ion channels largely determine the input/output relationships of electrically excitable cells. A variety of patch pipette voltage clamp techniques are available to characterize ionic currents. However, when used by themselves, such techniques are not well suited to the task of mapping low-density channel distributions. We describe here a new voltage clamp method (the whole cell loose patch (WCLP) method) that combines whole-cell recording through a tight-seal pipette with focal extracellular stimulation through a loose-seal pipette. By moving the stimulation pipette across the cell surface and using a stationary whole-cell pipette to record the evoked patch currents, this method should be suitable for mapping channel distributions, even on large cells possessing low channel densities. When we applied this method to the study of currents in cultured chick myotubes, we found that the cell cable properties and the series resistance of the recording pipette caused significant filtering of the membrane currents, and that the filter characteristics depended in part upon the distance between the stimulating and recording pipettes. We describe here how we determined the filter impulse response for each loose-seal pipette placement and subsequently recovered accurate estimates of patch membrane current through deconvolution.

INTRODUCTION

The signaling properties of electrically excitable cells are shaped, in large part, by the complement and distribution of ion channels within the plasma membrane. Therefore, to understand how a particular cell receives and responds to input, it is necessary to know the types of ion channels that the cell expresses and how the channels are distributed across its surface. Several techniques are available for identifying ionic currents in excitable cells, but the most widely used methods are not well suited to examining channel distribution. For example, tight-seal whole-cell recording techniques (Hamill et al., 1981; reviewed by Marty and Neher, 1995) permit the resolution of extremely small ionic currents, but they collect currents from the entire cell surface and therefore provide little information about the spatial distribution of the currents. Furthermore, voltage errors arising from poor space clamp of large cells, as well as the inability to completely compensate for the series resistance of the recording pipette (Armstrong and Gilly, 1992), typically limit this method to use with small cells having ionic currents of less than a few nanoamperes. The two-electrode voltage clamp method (reviewed in Smith et al., 1985) reduces the series resistance problems, and can thus be used to voltage-clamp cells with larger currents, but space-clamp problems limit the usefulness of these methods when they are used to study muscle cells or neurons with long processes, and again, these methods do not provide any infor-

mation on the spatial distribution of the current(s) being examined.

To overcome the lack of spatial resolution in whole-cell recording techniques, one can turn to patch clamp methodologies (Hamill et al., 1981; reviewed in Penner, 1995). However, when used by themselves, these methods also have their drawbacks. Although the tight-seal cell-attached patch method can be used to record from very small membrane areas (a few μm^2), constructing a spatial map of channel distribution from such recordings is not practical, because each pipette can be used only once, and quantitative comparisons of current density measurements from different pipettes are difficult, because of uncertainties in the patch areas (Sakmann and Neher, 1995). Furthermore, the generation of a tight seal and subsequent formation of a membrane bleb (omega figure) within the pipette cause massive local disruption of the cell membrane (Milton and Caldwell, 1990). The possible effects of seal formation on channel properties have not been adequately assessed, and could be substantial, particularly for channels that are regulated by cytoskeletal interactions.

A less widely used variant of the tight-seal cell-attached patch method uses large-bore pipettes, typically 12–40 μm in diameter (Hilgemann, 1995). This method overcomes some of the problems associated with sampling very small areas of membrane, but the damage inflicted by repeatedly sealing and removing large, tightly sealed pipettes makes multiple sampling with the giant membrane patch method untenable.

Another method for mapping ionic current distribution is the loose-seal patch clamp technique (Strickholm, 1961; reviewed in Roberts and Almers, 1992). In this method, a seal with low electrical resistance is formed between the cell and a large extracellular pipette (5–20 μm diameter). As in tight-seal recordings, the loose-seal pipette applies voltage

steps and measures the resulting patch current. Forming a low-resistance seal between the membrane and the pipette causes much less damage than forming a tight seal, and does not require the pipette and cell to be completely free of debris. Therefore a single pipette can be used to sample from multiple areas on a cell (or even from multiple areas of several different cells) with relatively little damage. However, the low electrical resistance of the seal makes these types of recordings inherently noisy and subject to artifacts. Lupa and Caldwell (1991) estimate that the resolution limit of this technique is ~1 mA/cm². In theory, one could use the loose-seal technique to record from cells with low densities of channels by simply increasing the size of the pipette, with the upper limit of the pipette bore being determined by the size of the cell. However, as discussed in Roberts and Almers (1992), achieving such resolution with the loose-seal patch clamp requires accurate leak compensation (both analog and digital) and signal averaging. Thus the loose-seal patch clamp has proved useful for looking at current and channel distribution over cells that are specialized to generate fast action potentials (Almers et al., 1983; Caldwell et al., 1986; Roberts, 1987), but it has not been useful for examining current distribution on cells in which current densities are much lower, particularly developing cells (Lupa and Caldwell, 1991; Anson and Roberts, 1994).

Elucidating the current distribution over immature, electrically excitable cells and how this distribution changes throughout development will shed light on how the mature current phenotype is achieved and maintained. Such knowledge, in turn, will enable a better understanding of the pathology underlying developmental abnormalities and disease states affecting electrically excitable cells. To measure current distributions on developing myotubes, we have modified and refined techniques that were used to map ionic currents on taste receptors (Kinnamon et al., 1988) and hair cells (Roberts et al., 1990) for use on larger cells. Our technique uses a tight-seal whole-cell pipette to record ionic currents elicited by focal stimulation through a loose-seal patch pipette (the WCLP technique; Fig. 1). By using the advantages of one technique to discount the disadvantages of the other, i.e., by using a loose-seal stimulating pipette to overcome sampling problems associated with tight-seal patch pipettes, and a tight-seal whole-cell recording pipette to counter the low resolution of the loose-seal pipette, we are able to accurately map low-density currents from large cells. In our initial experiments using the WCLP technique, we discovered that the cable properties of the muscle cell, acting in concert with the uncompensated series resistance of the whole-cell recording pipette, comprised a low-pass electrical filter with complex temporal characteristics that varied among cells and changed as the stimulating pipette was moved along the myotube. This filter slowed and attenuated the Na^+ currents that we recorded, which, if taken at face value, would result in a large underestimation of
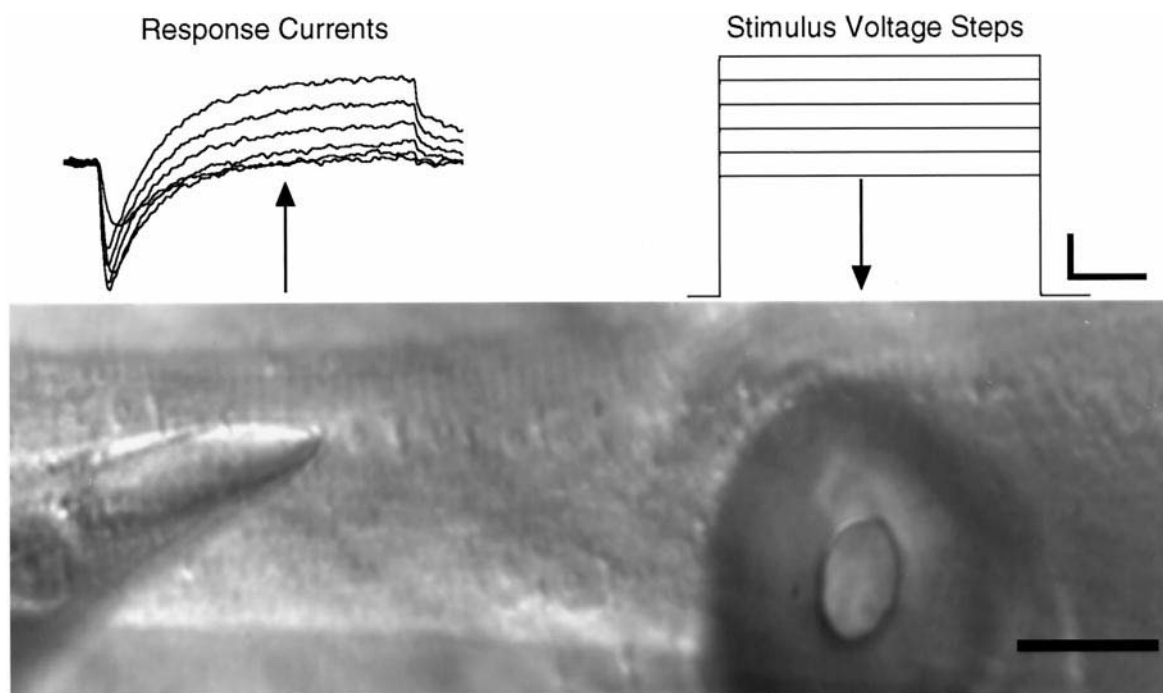

FIGURE 1 The WCLP technique. Ionic currents (*group of traces in the upper left*) recorded by a tight-seal whole-cell pipette in response to depolarizing voltage steps (*rectangulular waveforms in the upper right*) focally applied by a loose-seal patch pipette to the patch of myotube membrane directly beneath the tip of the pipette. The patch pipette rim is the roughly elliptical profile on the right-hand side of the lower micrograph. The currents were stimulated extracellularly through the loose-seal pipette and recorded intracellularly through a whole-cell pipette (*smaller pipette on the left-hand side of the lower micrograph*). Ionic currents were recorded and processed as described in Methods and Materials. The upper scale bar represents 50 pA or 20 mV (*vertical*) and 5 ms (*horizontal*). The lower scale bar is 25 μm.

current and channel densities, as well as inaccurate comparisons between patches. This paper describes the WCLP technique, including the method that we designed to characterize the filter properties of the cell and recording pipette, and the deconvolution procedure by which the unfiltered currents were recovered. When carefully applied, the WCLP technique should be useful for exploring the distribution of ion channels from muscle and other large, electrically excitable cells.

MATERIALS AND METHODS

Cell culture

Primary cultures of myotubes were prepared following the general procedures of Fischbach et al. (1971). Briefly, pectoral muscles of day 11–13 embryonic chickens were dissected, mechanically dissociated, and incubated in a solution of 5 ml Puck's saline and 2 ml 0.09% trypsin (Gibco, Grand Island, NY) at 37°C for 10 min. The cell slurry was centrifuged, and the resulting pellet resuspended in plating media composed of minimum essential medium supplemented with glutamate (Gibco), 10% heat-inactivated horse serum, 5% chick embryo extract, 50 units/ml penicillin, and 50 μg/ml streptomycin. Myoblasts were plated in 1.4 ml of media at a density of 1×10^5 cells/ml in 35-mm plastic petri dishes coated with Matrigel (Becton-Dickenson, Bedford, MA) at a dilution of 1:50. Cultures were maintained at 37°C in a 95% ambient air/5% CO_2 atmosphere. Between 24 and 48 h after culture establishment, plating medium was replaced with medium containing 10 μM cytosine arabinofuranoside (Ara-C) and 2% chick embryo extract. The medium was replaced 24 h later with 2% chick embryo extract medium without Ara-C. Medium was changed every other day thereafter. Myotubes reached their adult morphology after 3–4 days in culture.

Electrophysiology set-up

Whole-cell recordings were made using an Axopatch 1C voltage clamp (Axon Instruments, Foster City, CA), and loose-seal patch stimulation was performed with a voltage clamp designed by W. Roberts (Roberts and Almers, 1992). Both whole-cell and loose-patch pipettes were made from R6 soda-lime glass (Garner Glass Co., Claremont, CA) coated with silicon-elastomer (Sylgard type 184; Dow Corning, Midland, MI) to reduce the apparent pipette capacitance, and then heat-polished. Pipette capacitance was electronically compensated after the pipette was sealed to the cell membrane. Electrical connections to the whole-cell and loose-seal pipettes were made through chloride-coated silver wires. In the case of the loose-seal pipette, two wires were used, one serving as a voltage reference electrode, and the other passed the stimulus current. The bath was grounded using separate voltage-sensing and current-passing electrodes connected to a feedback circuit that clamped the bath at the ground reference potential of the whole-cell voltage clamp. Both bath ground connections were made through chlorided silver wires and agar bridges. This active ground greatly reduced, but did not completely eliminate, the stimulus artifact produced by the large current emanating from the loose-seal patch pipette (see below). All voltage commands, both whole-cell and loose-seal, were made relative to the whole-cell voltage clamp reference potential.

Whole-cell pipettes were filled with internal saline composed of (in mM) 140 KCl; 1 $CaCl_2$; 2 $MgCl_2$; 10 EGTA; 10 HEPES; pH was adjusted to 7.35 with KOH. The loose-seal patch pipette was filled with external saline composed of (in mM) 127 NaCl; 4.4 KCl; 3 $CaCl_2$; 1 $MgCl_2$; 11 glucose; 10 HEPES; 30 TEA-Cl. The pH was adjusted to 7.35 with NaOH. All chemicals were obtained from Sigma (St. Louis, MO).

All electrical recordings were made at room temperature on the stage of a Zeiss Axiovert microscope. Images of cells and electrode placements used for subsequent analysis were obtained with a Pulnix CCD camera driven by Image-1 software.

Whole-cell recording, loose-seal stimulation, and subtraction of the stimulus artifact

In all experiments, the whole-cell command potential (V_c) was −100 mV, but the actual intracellular potential was somewhat more depolarized, because of the low input resistance (R_{input}) of the myotube and the inability to completely compensate for the series resistance of the whole-cell pipette. The membrane potential near the tip of the whole cell pipette is

$$V_{intracellular} = (V_c \cdot R_{input} + V_{rest} \cdot R_{series})/(R_{input} + R_{series}),$$
(1)

where V_{rest} is resting membrane potential and R_{series} is the uncompensated portion of the series resistance. R_{series} varied between 10% and 100% of R_{input}. Therefore, assuming a resting potential of approximately −60 mV (Fischbach et al., 1971), $V_{intracellular}$ ranged between −80 and −96 mV. Because of the cable properties of the myotubes under investigation, $V_{intracellular}$ approached the resting membrane potential with increasing distance away from the whole-cell pipette. However, given the reported estimates of the space constant (λ) for these cells (Fischbach et al., 1971), the separation between the whole-cell and loose-seal electrodes was less than $\lambda/3$. Thus $V_{intracellular}$ was relatively constant over the area of membrane examined.

Once tight-seal whole cell recording was established, the loose-seal patch pipette was positioned above the myotube and lowered until contact between the pipette rim and cell membrane formed an electrical resistance that partially insulated the patch of membrane encompassed by the loose-seal pipette rim from both the bath and the rest of the cellular membrane. The resistances of the loose-seal pipette and seal were determined from the current response to small depolarizations before and after the pipette contacted the cell, and were electronically nulled as described by Roberts and Almers (1992). The loose-seal resistance was always greater than twice the pipette resistance.

For unknown reasons, the low-resistance seal between the pipette and cell membrane does not obey Ohm's law precisely. Although the series resistance compensation circuitry of the loose-seal voltage clamp did not assume an ohmic seal, and could maintain the correct command potential at the pipette tip under these conditions (see Roberts and Almers, 1992), the nonideal behavior of the seal greatly reduced the effectiveness of leak subtraction procedures used to separate membrane currents from seal currents. The nonideal behavior of the loose seal was the major limiting factor that we encountered when attempting to resolve small membrane currents in loose patch recordings, and was thus the main impetus for the development of the WCLP method. By measuring patch currents through a separate whole-cell recording pipette, the requirements for leak subtraction were greatly reduced.

Patch currents were elicited using a series of 15-ms depolarizing voltage steps delivered by the loose-seal voltage clamp. Each series of depolarizations consisted of voltage steps to 60, 70, 80, 90, 100, 110, and 120 mV relative to $V_{intracellular}$. The resulting patch currents recorded by the whole-cell voltage clamp were filtered at 5 kHz (−3-dB cutoff frequency) before being digitized at a sampling rate of 25 kHz and stored as the averaged response to 15 series of depolarizations. The interstep time (start to start) was 100 ms, and the interseries time (start to start) was 1 s. Patch membrane currents that scaled linearly with voltage were removed from the records by subtracting an appropriately scaled subthreshold response. All data acquisition was done with pClamp software (Axon Instruments), and off-line analysis was done within Clampfit (Axon Instruments), Excel spreadsheets (Microsoft), and Igor (Wavemetrics).

As previously mentioned, the series resistance of the whole-cell pipette (R_{series}) varied between R_{input} and $R_{input}/10$. Thus the whole-cell pipette collected only 50–90% of the low-frequency components of the total membrane current, and a smaller fraction of the high-frequency components. The rest of the current escaped to ground through the input imped-

ance of the cell. To compensate for the low-frequency attenuation, whole-cell recordings of patch currents were multiplied by the factor $1 + (R_{series}/R_{input})$, where R_{series} was calculated as V_{step}/I_0, and I_0 was the current extrapolated to time 0 in response to a small whole-cell voltage step of magnitude V_{step}. High frequencies were recovered using the deconvolution procedure described below.

When the loose-seal pipette was on the cell, with pipette and seal resistances compensated as described by Roberts and Almers (1992), small voltage steps applied by the loose-seal patch clamp (i.e., within the linear voltage range of the myotube) produced a whole-cell current waveform comprising a stimulus artifact (I_{art-on}), current charging the patch capacitance (I_{cap}), and current flowing through the patch resistance (I_{res}):

$$I_{wc-on} = I_{art-on} + I_{cap} + I_{res}. \tag{2}$$

For most purposes the stimulus artifact was not problematic, because it was of short duration and was removed along with I_{cap} and I_{res} during the leak subtraction procedure used to separate voltage-gated currents from passive currents. However, the deconvolution procedure described in the Results required that we determine I_{cap} and I_{res}. To do this we had to first determine and subtract I_{art-on}.

We found that I_{art-on} was composed of two components. One component was independent of the position of the loose-seal pipette relative to the myotube. We believe that this component was caused by current flowing through the small but nonzero resistance of the bath ground, and possibly by capacitive coupling between the loose-seal and whole-cell pipettes. The second component, which increased as the loose-seal pipette approached the muscle cell, was caused by the field potential around the tip of the pipette. Although the field potential was small compared to the voltage steps applied to the patch of membrane beneath the pipette tip, it enveloped a large area of myotube membrane and thus evoked a measurable membrane current. By using parameters typical of a WCLP experiment, a rough estimate of the magnitude of the field potential effect can be obtained by calculating the capacitive artifact associated with the charge (Q) that moves onto the membrane capacitance as a result of the field potential (V_{field}) created when a command potential (V) is applied to the tip of the loose patch pipette. This artifact can be expressed as an "apparent" capacitance: $C_{app} = Q/V$. The approximate magnitude of C_{app} as seen through the whole-cell recording pipette is determined by integrating the charge movement per unit length of myotube ($C_l V_{field}$), over a distance of one space constant (λ) in both directions: $Q \approx 2\int_a^\lambda C_l V_{field} \, dr$, where a ($\approx 10 \, \mu$m) is the pipette radius and C_l is the capacitance per unit length of the myotube. Typically, $C_l \approx 2$ pF/μm for a myotube with a circumference of 50 μm and a specific membrane capacitance of 4 μF/cm^2. The field potential is proportional to V and inversely proportional to the distance (r) from the pipette: $V_{field} \approx (Va/r) \cdot (R_{access}/(R_{access} + R_{seal}))$, where $R_{seal} \approx 500$ kΩ is the resistance of the loose seal and $R_{access} \approx \rho/4a$ (Hille, 1992, p. 296) is the resistance from the pipette to ground through the bathing medium of resistivity, $\rho \approx 100 \, \Omega \cdot$ cm. Note that in most cases R_{seal} is much greater than R_{access}, and thus $R_{access}/(R_{access} + R_{seal})$ is essentially equivalent to R_{access}/R_{seal}. Substituting the expressions for V_{field}, C_{app}, and R_{access}, then integrating over r, gives $C_{app} \approx (\rho C_l/2R_{seal}) \cdot \ln(\lambda/a) \approx 2$ pF $\cdot \ln(\lambda/a)$. Thus, for a myotube with $\lambda = 600 \, \mu$m, $C_{app} \approx 8$ pF, which is a substantial fraction of the patch capacitance and therefore needs to be removed before the deconvolution process is begun.

To determine I_{art-on}, we made use of the fact that the artifact was largely the result of (and proportional to) current supplied by the loose-seal patch clamp acting at a distance from the pipette tip, and thus did not change significantly as the loose-seal pipette was moved the final few microns before sealing to the myotube. Although formation of the loose seal reduced the amplitude of the artifact in proportion to the reduction in current flowing to ground, the waveform is not expected to change significantly. Thus we could determine the waveform of I_{art-on} by recording and scaling the stimulus artifact ($I_{art-off}$) generated with the loose-seal pipette positioned a few microns above the myotube.

With the loose-seal pipette off the myotube and the pipette resistance compensation not engaged, the total current emanating from the loose-seal pipette depends upon the command voltage ($V_{loose-seal}$) and the pipette

resistance (R_{pip}): $I_{off} = V_{loose-seal}/R_{pip}$. After measuring $I_{art-off}$, we lowered the pipette the final few microns onto the myotube to form a loose seal with a resistance of R_{seal} and engaged the compensation for the pipette and seal resistances, so that the total current emanating from the loose-seal pipette was now $I_{on} = V_{loose-seal}/R_{seal}$. Thus

$$I_{on}/I_{off} = R_{pip}/R_{seal}. \tag{3}$$

Because the amplitude of artifact is also proportional to I_{on}/I_{off}, we have

$$I_{art-on}/I_{art-off} = R_{pip}/R_{seal}. \tag{4}$$

Values for R_{pip} and R_{seal} were determined for each pipette and seal. Rearranging Eq. 4 then allows calculation of I_{art-on} as a scaled version of $I_{art-off}$:

$$I_{art-on} = I_{art-off}(R_{pip}/R_{seal}). \tag{5}$$

Subtracting the stimulus artifact from both sides of Eq. 2 gives

$$I_{wc-on} - I_{art-off}(R_{pip}/R_{seal}) = I_{cap} + I_{res}. \tag{6}$$

The left-hand side of Eq. 6 is a measured quantity, which we determined for each placement of the loose-seal pipette. Thus we were able to separate I_{art-on} from the sum of I_{cap} and I_{res}. The subsequent separation of I_{cap} from I_{res} and filter deconvolution is described in the Results.

RESULTS

Recording ionic currents with the WCLP method

Combining tight-seal whole-cell recording with loose-seal patch stimulation allows one to stimulate and record ionic currents from discrete areas of large cells, even when the current density is low. Fig. 1 illustrates this method as applied to cultured skeletal myotubes. A whole-cell pipette (*left side* of Fig. 1) was used to record ionic currents flowing in response to extracellularly applied depolarizing potentials from a loose-seal patch pipette, the rim of which is visible as the roughly elliptically shaped profile on the right-hand side of Fig. 1. Voltage steps applied by the loose-seal patch pipette are illustrated above the rim profile, and the resulting leak subtracted currents (see Materials and Methods) are shown above the whole-cell electrode. Because cultured myotubes are highly flattened in cross section, loose-seal pipettes were bent such that they approached from directly above the cell. The vertical orientation was necessary to obtain uniform contact between the pipette rim and cell surface and to aid in visualization of the pipette rim. The magnitude of the voltage steps shown here and elsewhere are relative to $V_{intracellular}$, with the standard sign convention of

$$V_{patch} = V_{intracellular} + V_{loose-seal}, \tag{7}$$

with $V_{intracellular}$ and $V_{loose-seal}$ as previously defined (Materials and Methods). Current traces follow the convention of inward denoted as negative and outward denoted as positive.

In the ideal situation of a perfect whole-cell voltage clamp (i.e., no uncompensated series resistance in the whole-cell pipette, infinite membrane space constant, and zero extracellular resistivity), only the membrane patch beneath the loose-seal pipette would experience a change in

membrane potential. Therefore the whole-cell current would equal the current flowing through the membrane encompassed within the rim of the loose-seal patch pipette.

In the actual recording situation, the effects of the non-ideal whole-cell voltage clamp must be removed to obtain accurate recordings of membrane current. Fig. 2 compares currents recorded from a large myotube via the WCLP method (Fig. 2, *A* and *C*) with whole-cell currents recorded from a small isopotential myoblast (Fig. 2, *B* and *D*). Note that the patch Na^+ current (Fig. 2 *A*) recorded from the large

FIGURE 2 Na^+ currents recorded with the WCLP method are filtered. Families of Na^+ currents were recorded from a large myotube by the whole-cell/loose-patch method (*A*) and, for comparison, from a small isopotential myoblast, using a conventional whole-cell voltage clamp (*B*). The Na^+ currents are much slower in the myotube recording than in the myoblast recording. These kinetic differences can be explained by the slowness of the myotube voltage clamp and by the cable properties of the myotube, as demonstrated by the slowness and multiple exponential decay of the capacitative transient in the myotube's linear step response (*C*) compared to the fast transient from the myoblast (*D*). Na^+ currents in *A* and *B* were elicited in response to depolarizing command potentials of 60–120 mV in increments of 10 mV from a holding potential of −100 mV. Depolarizations were applied through the loose-seal (*A*) or whole-cell (*B*) pipette. Linear currents were removed through leak-subtraction procedures (Materials and Methods). The linear step responses of the myotube (*C*) and myoblast (*D*) were recorded in response to a depolarizing 10-mV command potential.

myotube is slower than the whole-cell Na^+ current recorded from the myoblast (Fig. 2 *B*). The slow kinetics of the patch current can be explained by the slowness of the myotube whole-cell voltage clamp and the cable properties of the myotube (Fig. 3), which act to electrically filter the patch current, as demonstrated by the slow decay of the capacitive transient from the myotube's linear step response (Fig. 2 *C*), compared to the fast transient step response of the myoblast (Fig. 2 *D*).

Although it is not evident from Fig. 2, filtering of the patch current also decreases the apparent magnitude of the peak current. Therefore, if one desires to compare patch currents between myotubes or even from different areas of the same myotube, the original current waveform needs to be recovered. Recovery of the original Na^+ current waveform and magnitude can be achieved by first characterizing the filter elements acting on the current waveform, and then using that characterization to deconvolve the filtered Na^+ current.

Filter characterization

After removal of the stimulus artifact (Materials and Methods), the whole-cell current waveform consisted of patch currents that have been electrically filtered by the electrotonic properties of the myotube and whole-cell pipette. Fig. 3 shows a schematic of the myotube, pipettes, whole cell, and patch currents, and the passive filter elements of the preparation. In response to a small voltage step within the linear range of the myotube membrane (V_{step}; Fig. 3) delivered by the loose-seal patch clamp, the whole-cell pipette recorded a transient current that declined to a steady level (step response; Fig. 3). Because the stimulated patch comprised a small fraction of the total cell surface, the passive current that flowed across the patch caused a very small perturbation of the intracellular potential relative to V_{step}. Therefore, the patch experienced a nearly stepwise change in membrane potential, resulting in an instantaneous capacitive transient (I_{cap}) and a stepwise resistive current (I_{res}). These currents were then electrically filtered by the cable properties of the cell (r_m, c_m, and r_i) and the uncompensated series resistance of the whole cell recording pipette (R_{series}) to produce the step response recorded by the whole-cell pipette.

Because R_{series} and the cable properties of the myotube are passive and assumed to be temporally constant, one is justified in presuming that the filter comprising the previously mentioned components is linear. A linear filter can be characterized by the manner in which it affects an impulse (an input of infinite amplitude and infinitesimal duration) applied to its input, i.e., a linear filter is characterized by its impulse response ($I_{impulse}$). Because any time-varying input can be approximated by a series of closely spaced impulses of different amplitudes (Jack et al., 1983), the output of a linear filter is simply the sum, or superposition, of the responses to all of the impulses making up the input. This
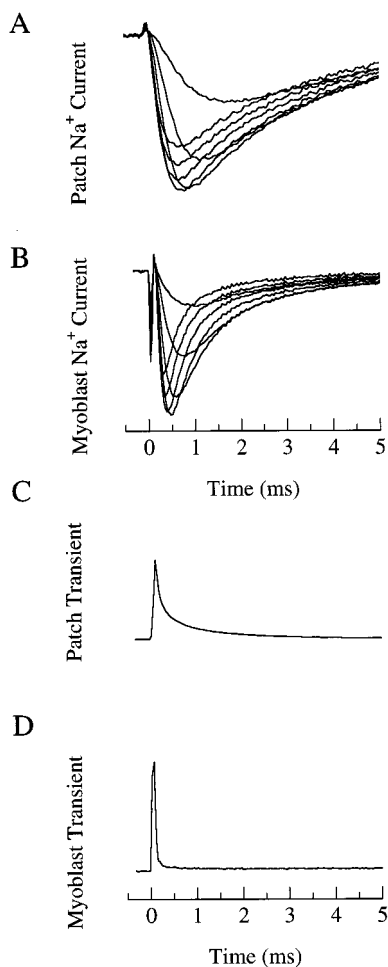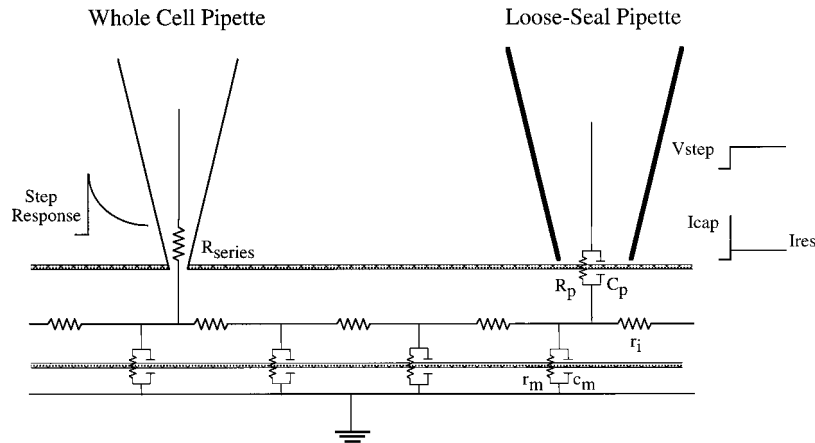
FIGURE 3 Schematic of the filter components of the WCLP recording set-up. When the loose-seal patch clamp applies a small rectangular voltage step (V_{step}) within the linear range of the membrane, the initial current (I_{cap}) charges the capacitance of the membrane encompassed within the bore of the loose-patch pipette (C_p), and the sustained current (I_{res}) flows through the resistance of the patch membrane (R_p). I_{cap} and I_{res} are electrically filtered by the combination of the cable properties of the cell (r_i, r_m, and c_m) and the uncompensated series resistance of the whole-cell pipette (R_{series}). The whole-cell pipette thus records (after subtraction of the stimulus artifact; see text) a step response that is the sum of the filtered capacitive and resistive patch currents. Because of the linearity of the filtering elements, whole-cell recordings of Na^+ currents flowing through the patch of membrane beneath the loose-seal pipette in response to larger depolarizations are filtered in the same way as I_{cap}.

type of superposition is described mathematically as convolution: the output of a linear filter is the convolution of the input with the filter's impulse response. The convolution operation, and more importantly for this work, its inverse (i.e., deconvolution), are most easily performed in the frequency domain as simple multiplication (McGillam and Cooper, 1991). Thus, if $Na^+_{unfiltered}$ is the true waveform of a Na^+ current flowing through the stimulated membrane patch, then

$$F[Na^+_{filtered}] = F[Na^+_{unfiltered}] \times F[I_{impulse}], \qquad (8)$$

where $F[]$ represents the Fourier transform operation, and $Na^+_{filtered}$ is the filtered waveform of the Na^+ current recorded by the whole-cell pipette in response to patch stimulation by the loose-seal voltage clamp. Deconvolution is accomplished in the frequency domain by division:

$$F[Na^+_{unfiltered}] = F[Na^+_{filtered}]/F[I_{impulse}]. \qquad (9)$$

Thus the inverse Fourier transform of the ratio of the Fourier transform of the filtered Na^+ current over the Fourier transform of the impulse response equals the unfiltered Na^+ current. Therefore, to recover the unfiltered Na^+ currents from each patch recording, the impulse response of the filter must be determined for each recording.

Determining the impulse response

As illustrated in Fig. 4, *A* and *B*, the linear step response (I_{step}) recorded by the whole-cell pipette equals the sum of the filtered patch capacitive and resistive currents: $I_{step} = I_{cap} + I_{res}$. In the following description, I_{step} is the waveform of the step response after the stimulus artifact is removed (i.e., I_{step} is the left-hand expression in Eq. 6). Because the loose-seal patch clamp charges the patch capacitance in less

than one-tenth the filtering time constant imposed by the recording electrode and myotube cable properties, the capacitive patch current is equivalent to an impulse (McGillam and Cooper, 1991), and I_{cap} thus represents the impulse response of the filter. Therefore, once I_{step} is broken down into its component capacitive and resistive currents, I_{cap} can be used to deconvolve the filtered Na^+ currents using Eq. 9.

The linear step response was broken down into its component resistive and capacitive currents by an iterative curve fitting procedure that relied upon two important properties of I_{cap} and I_{res}. The first important property is that the waveform of I_{cap} can approximated by Green's function for the cable equation (Rall, 1977):

$$G(X, T) = T^{-1/2}\exp(-X^2/4T - T) \qquad (10)$$

$G(X, T)$ specifies the filtering of an impulse along a cable in terms of normalized time ($T = t/\tau$) and electrotonic distance ($X = x/\lambda$), where τ is the membrane time constant, λ is the cable space constant, and x is the distance between the two electrodes. Because the rising phase of I_{cap} is extremely rapid, the effects of the whole-cell voltage clamp filter setting must be taken into account. Therefore, the Green's function was convoluted with a Gaussian function ($B(t)$), approximating the whole-cell voltage clamp's Bessel filter, to give the normalized waveform (I_c) of the filtered capacitive transient,

$$I_c = G(X, T) * B(t), \qquad (11)$$

where $B(t) = \exp((t - d)^2/\sigma^2)$, d is the Bessel filter's time delay, and σ specifies the bandwidth (-3-dB cutoff frequency of 5 kHz). To calculate I_{cap}, one must also determine a scale factor (A_{cap}) that reflects the magnitude of the patch capacitance:

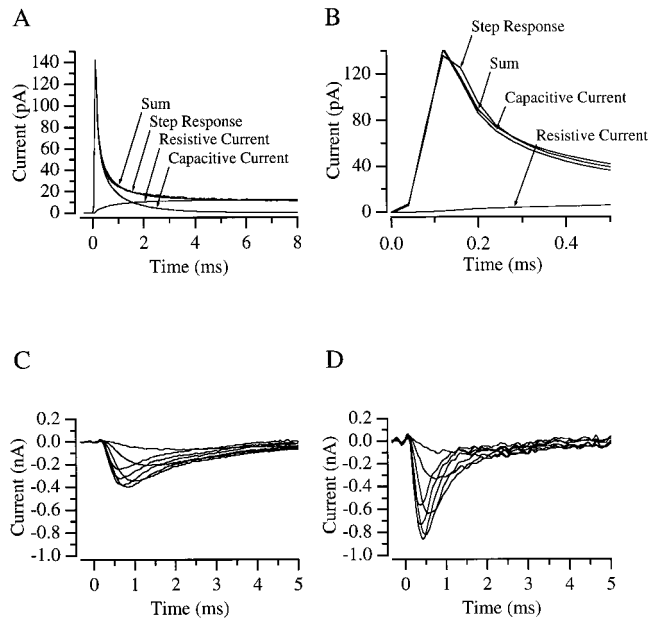$$I_{cap} = A_{cap}I_c. \qquad (12)$$

FIGURE 4   The linear step response of each loose-patch/whole-cell recording was used to determine the linear filter properties of the system for each patch, and then to correct the recorded Na$^+$ currents by deconvolution. (*A*) I_{cap} and I_{res} of Fig. 3 were separated from each other during the step response, using the fitting procedure described in the text, to yield the filtered capacitive current and filtered resistive current, the sum of which is a good fit to the step response. (*B*) Expanded time scale of *A*. (*C*) Na$^+$ currents before deconvolution. The recording set-up is as described in Materials and Methods. (*D*) Deconvolved Na$^+$ currents, computed using the capacitative current shown in *A* as the filter's impulse response (see text). After deconvolution, Na$^+$ currents were much larger than before, and as fast as the Na$^+$ currents recorded from small myoblasts (Fig. 2 *B*).

Equations 10–12 yield only an approximation to I_{cap}, because the Green's function did not take into account the R_{series} of the whole-cell recording pipette. The fitting procedure thus does not give meaningful estimates of T or X. However, the form of I_{cap} obtained using the simple Green's function shown in Eq. 10 was very similar to the form obtained using a more complex equation that included R_{series}. Because fitting the more complex equation was extremely time consuming and did not yield noticeably different results, we used Eq. 10 for most deconvolutions.

The second important property was that the normalized waveform (I_r) of the resistive current is the time integral of I_c (i.e., a step is the time integral of an impulse). The goal of the fitting procedure was thus to find values of the cable parameters (X and T), plus two scale factors (A_{res} and A_{cap}) that minimized the mean squared error:

$$|I_r A_{res} + I_c A_{cap} - I_{step}|^2 = \min. \tag{13}$$

For this digital computation, $I_r(t)$, $I_c(t)$, and $I_{step}(t)$ were each considered to be 512 point column vectors. For ease of computation, Eq. 13 was reformulated as a single matrix equation:

$$|M \cdot A - I_{step}|^2 = \min,$$

where M is a 512×2 matrix in which the columns are I_c and I_r, and A is a 2×1 matrix, in which the elements are A_{cap} and A_{res}. The values of A_{cap} and A_{res} that minimize Eq. 13 are then given by

$$A = (M^T M)^{-1} M^T I_{step}, \tag{14}$$

where M^T is the transpose of M.

The fitting process began with initial guesses of X and T, from which I_c was calculated from Eqs. 10–12. I_r was then calculated by numerical integration of I_c, and Eq. 14 was applied to find the best-fit values of A_{cap} and A_{res}. Using these values of A_{cap} and A_{res}, new best-fit values of X and T were then found using the search algorithm built into the EXCEL spreadsheet program. The process was then iterated, alternating between finding the best values of A_{cap} and A_{res} using matrix inversion (Eq. 14) and best values of X and T using EXCEL's search algorithm, until a criterion was satisfied. The end result is illustrated in Fig. 4, *A* and *B*, where the step response has been broken down into its resistive and capacitive currents, the sum of which is a good fit to the step response.

Deconvolution of the attenuated and slower filtered Na$^+$ current (Fig. 4 *C*) with the capacitive component of the step response results in current waveforms (Fig. 4 *D*) greater in magnitude and with kinetics resembling those of Na$^+$ currents recorded from isopotential myoblasts (for a comparison see Fig. 2 *B*).

Deconvolution procedure and checks

Once the impulse response has been separated from the step response, 512-point discrete Fourier transforms (DFT) of the impulse response and filtered Na$^+$ current are calculated and used to deconvolve the filtered Na$^+$ current as expressed in Eq. 4. We calculated the DFT by matrix multiplication (James, 1995); a minor time savings could be realized by using a fast Fourier transform algorithm. The deconvolution process produces representations of unfiltered Na$^+$ current with an unacceptable amount of high-frequency noise; therefore the deconvolved currents are digitally filtered to remove high-frequency noise. The actual process of filtering is accomplished in the frequency domain through multiplying the impulse response DFT by a Gaussian filter with a 2.5-kHz half-power cutoff frequency. This operation did not grossly alter the overall power distribution of either the impulse response or the unfiltered Na$^+$ current waveform, because, as illustrated in Fig. 5 *A*, most of the power in these two waveforms is contained within frequencies below 2.5 kHz (89% for the impulse response and 88% for the myoblast Na$^+$ current).

Fig. 5 *B* shows the effect filtering the impulse response DFT has on the deconvolved Na$^+$ current waveform. If myoblast Na$^+$ channels are similar to those of myotubes, then the convolution of myoblast Na$^+$ current with a typical impulse response from a myotube should produce currents similar to those recorded by the WCLP method. As illus-
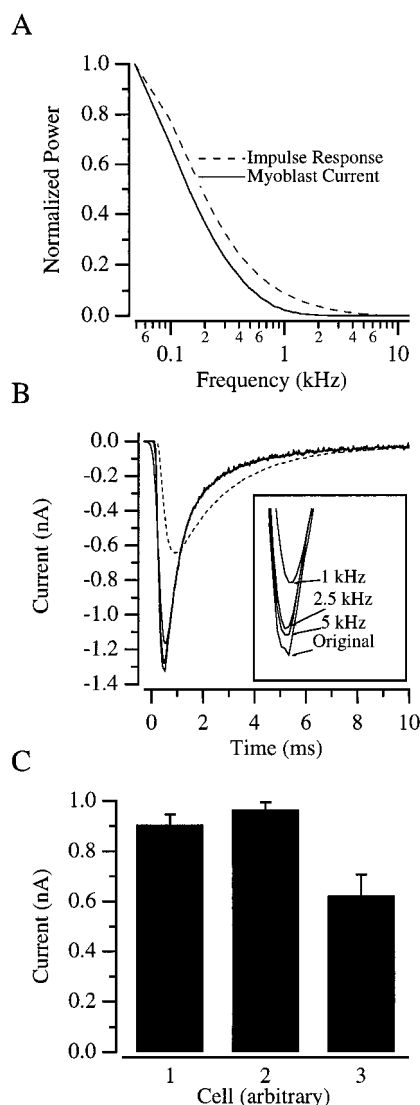
A

B

C

FIGURE 5   Determination of the cutoff frequency used in the deconvo-lution procedure and reproducibility of the deconvolution prodedure. (*A*) The power spectrum of a typical impulse response from a loose-patch/ whole-cell recording from a myotube (– – –) and Na$^+$ current recorded from a myoblast (——) reveal substantial attenuation at frequencies above 2.5 kHz. Both curves have been normalized, so their DC power is equal to one. (*B*) Convolution of myoblast Na$^+$ current with a typical impulse response. If myotube Na$^+$ channels are similar to those on myoblasts, then the Na$^+$ current waveform in whole-cell/loose-patch recordings is the convolution of the fast myoblast waveform (*trace with the largest peak amplitude, labeled original in the blow-up shown in the inset*) with the myotube impulse response. This convolution yields a slowed and attenu-ated waveform (– – –) that indeed resembles the Na$^+$ currents recorded from myotubes (see also Figs. 1 and 2 *A*). Ninety-five percent of the original waveform's amplitude can be recovered by deconvolution, with the high-frequency cutoff set at 2.5 kHz (*B, inset*; the cutoff frequency is the half-power frequency of a Gaussian filter applied to the deconvoluted waveform). (*C*) Reproducibility of the deconvolution procedure. Mean and standard deviation of the peak amplitudes of deconvolved Na$^+$ currents obtained in repeated recordings from single patches. After each recording, the loose-patch pipette was lifted off the myotube and then placed back on the same spot for the next stimulation. Coefficients of variation for current recordings from patches 1, 2, and 3 are 4.4%, 2.9%, and 13.7%, respec-tively (*N* = 6, 5, 6).

trated in Fig. 5 *B*, this convolution does indeed yield a slower and attenuated waveform (Fig. 5 *B*, *dashed line*) similar to the filtered Na$^+$ current waveform recorded with the WCLP method (see Fig. 4 *C* for a comparison).

Fig. 5 *B* also shows the effect of smoothing the impulse response DFT at different cutoff frequencies. When the convolved myoblast current (*dashed line*) is deconvolved with the impulse response that has been smoothed at 1-kHz, 2.5-kHz, or 5-kHz cutoff frequency, one sees that the de-convolved currents more closely approximate the value of the original myoblast current. The cutoff value of 2.5 kHz was chosen because it significantly decreased the amount of noise in the deconvolved currents while still returning a value that was at least 95% of the original. Therefore the deconvolution process is accurate.

Experiments examining the precision of the WCLP method are illustrated in Fig. 5 *C*, which shows the results of multiple recordings obtained from single patches of membrane. In this experiment the loose-seal patch pipette was lifted off the myotube after each stimulation and then placed back on the same spot. This process was repeated several times for three different patches of membrane. Each bar thus represents the mean ($\pm$ SD) peak deconvolved current obtained from the multiple recordings from each of three patches. The mean current value for each patch was 0.91, 0.97, 0.62 nA, with coefficients of variations of 4.4%, 2.9%, 13.7%, respectively (*n* = 6, 5, 6). Thus, not only is the WCLP method accurate, it is also reasonably precise.

DISCUSSION

We have designed a technique that allows the mapping of a low-density current distribution on embryonic skeletal mus-cle cells in culture. Specifically, a tight-seal whole-cell pipette is used to record ionic currents elicited by focal stimulation through a loose-seal patch pipette. By using the loose-seal pipette to stimulate multiple areas of the cell surface, one can generate a spatial map of current density. The uncompensated series resistance of the whole cell pi-pette (R_{series}) and the cable properties of the myotube elec-trically filter the patch currents, making Na$^+$ current wave-forms appear slower and smaller. Because a portion of the filtering is due to the cell cable properties, which vary with separation between the whole-cell and loose-seal pipettes, comparisons between filtered currents from different cells, or even between patches on the same cell, are qualitative at best. To remedy this problem, we have developed a proce-dure to extract the filter impulse response by recording the current waveform in response to small steps. The impulse response can then be used to deconvolve the filtered patch current. The deconvolution process produces Na$^+$ current waveforms very similar to whole-cell Na$^+$ currents re-corded from small, spherical myoblasts. By repeatedly with-drawing and reapproaching the same patch, we found that the method yields Na$^+$ current amplitudes that are repro-ducible to within 5–15%.

As with other loose-seal methods, there is the possibility of "rim current" artifacts in WCLP recordings. This term refers to the current through ion channels located beneath the pipette rim, where the extracellular potential is intermediate between the loose-seal voltage command (V_{step}) and the bath potential. Channels in the rim region are not well voltage clamped, and contribute a poorly clamped rim current to the total patch current. Contamination of the recorded current by rim currents was the driving force for the development and use of concentric barreled pipettes with the loose-seal voltage clamp (Almers et al., 1983; Roberts and Almers, 1984) to accurately measure the amplitude and kinetics of the Na^+ current near its reversal potential, where the well-clamped patch current is small and the poorly clamped rim current is relatively large. The WCLP method does not alleviate problems introduced by rim currents. However, as previously shown by Almers et al. (1983; their figure 5) and Roberts and Almers (1984; their figure 7), even with a relatively low ratio of seal resistance to pipette resistance (1.5 and 1.7, respectively), significant distortion of Na^+ current occurs only at test potentials above 0 mV (e.g., during measurements of current reversal). At more negative test potentials, which evoke a large Na^+ current from the well-clamped channels, most rim channels are not sufficiently depolarized to open and thus do not contribute an artifact to the recorded current. Therefore the WCLP method is suitable for analysis of Na^+ current activation and peak Na^+ current magnitude at negative test potentials. If one wishes to examine patch currents at more extreme test potentials, rim currents can be minimized by using the whole-cell voltage clamp to hold the intracellular potential ($V_{intracellular}$) at a depolarized level to inactivate all Na^+ channels except those in the stimulated patch (Almers et al., 1983).

A second concern with the loose-seal patch clamp is the possibility that $V_{intracellular}$ may be significantly perturbed by the patch current (I_{patch}) flowing to ground across the input impedance (Z_{input}) of the cell. Our deconvolution procedure compensates for the loss of current across Z_{input}, but one also needs to consider whether the perturbation in $V_{intracellular}$ is large enough to influence the opening of voltage-gated channels. In an unclamped cell, the voltage perturbation ($\Delta V_{intracellular}$) produced by a steady patch current is $\Delta V_{intracellular} = I_{patch} \cdot R_{input}$. Transient patch currents that decay faster than the membrane time constant cause much smaller perturbations because a large part of the current flows onto the cell's input capacitance (Roberts and Almers, 1984). In our WCLP experiments, the perturbation was substantially reduced, although not completely eliminated, by the whole-cell voltage clamp. Under voltage clamp conditions, $\Delta V_{intracellular}$ at the tip of the whole-cell pipette (i.e., the voltage drop down the whole-cell pipette) is given by the product of the uncompensated series resistance (R_{series}) and the current flowing through the whole-cell pipette. In our data set of more than 200 WCLP recordings, this error was always less than 5 mV (average 1 mV; data not shown). The $\Delta V_{intracellular}$ at the stimulated patch could be substan-

tially greater than this if the distance between the whole-cell and loose-seal pipettes were large, but in our experiments the distance was less than $\lambda/3$. Thus both the stimulated patch and myotube membrane were well clamped in our experiments using cultured embryonic myotubes. The perturbations will be larger if one uses the WCLP method to study cells with higher current densities, but this increase can be countered by using a smaller diameter stimulating pipette.

In summary, through the addition of a whole-cell recording pipette, we have lowered the resolution limit for the loose-patch clamp to allow routine recording from embryonic myotubes with patch current densities as low as 0.2 to 0.5 mA/cm^2, which (assuming a peak single-channel current amplitude of ~1 pA and an open probability of 0.25 to 0.5; Schenkel and Sigworth, 1991) roughly corresponds to 4–20 channels/μm^2 of membrane. In practice, we have found that the deconvolution procedure described here works well as long as the input impedance of the cell under investigation is equal to or greater than the input impedance of the recording pipette. This technique should prove useful for examining the ways in which the mature current phenotype on skeletal muscle cells is generated and maintained. Furthermore, when appropriately modified, this method should also be useful for examining current distribution over other electrically excitable cells such as large neurons and large-diameter unmyelinated axons.

REFERENCES

Almers, W., P. R. Stanfield, and W. Stuhmer. 1983. Lateral distribution of sodium and potassium channels in frog skeletal muscle: measurements with a patch-clamp technique. *J. Physiol. (Lond.).* 336:261–284.

Anson, B. D., and W. M. Roberts. 1994. Sodium channel and acetylcholine receptor distributions on uninnervated embryonic skeletal muscle cells. *Soc. Neurosci. Abstr.* 363.14.

Armstrong, C. M., and W. F. Gilly. 1992. Access resistance and space clamp problems associated with whole-cell patch clamping. *Methods Enzymol.* 207:100–122.

Caldwell, J. H., D. T. Campbell, and K. G. Beam. 1986. Na channel distribution in vertebrate skeletal muscle. *J. Gen. Physiol.* 87:907–932.

Fischbach, G. D., M. Nameroff, P. G. Nelson. 1971. Electrical properties of chick skeletal muscle fibers developing in cell culture. *J. Cell. Physiol.* 78:289–300.

Hamill, O. P., A. Marty, E. Neher, B. Sakmann, and F. J. Sigworth. 1981. Improved patch-clamp techniques for high-resolution current recording from cells and cell-free membrane patches. *Pflugers Arch.* 391:85–100.

Hilgemann, D. W. 1995. The giant membrane patch. *In* Single-Channel Recording. B. Sakmann and E. Neher, editors. Plenum, New York. 307–327.

Hille, B. 1992. Ionic Channels of Excitable Membranes. Sinauer Associates, Sunderland, MA.

Jack, J. J. B., D. Noble, and R. W. Tsien. 1983. Electric Current Flow in Excitable Cells. Oxford University Press, Oxford.

James, J. F. 1995. A Student's Guide to Fourier Transforms. Cambridge University Press, Cambridge.

Kinnamon, S. C., V. E. Dionne, and K. G. Beam. 1988. Apical localization of K^+ channels in taste cells provides the basis for sour taste transduction. *Proc. Natl. Acad. Sci. USA.* 85:7023–7027.

Lupa, M. T., and J. H. Caldwell. 1991. Effect of agrin on the distribution of acetylcholine receptors and sodium channels on adult skeletal muscle fibers in culture. *J. Cell. Biol.* 115:765–778.

Marty, A., and E. Neher. 1995. Tight-seal whole-cell recording. *In* Single-Channel Recording. B. Sakmann and E. Neher, editors. Plenum, New York. 31–52.

McGillam, C. D., and G. R. Cooper. 1991. Continuous and Discrete Signal and System Analysis. Oxford University Press, New York.

Milton, R. L., and J. H. Caldwell. 1990. How do patch clamp seals form? A lipid bleb model. *Pflugers Arch. Eur. J. Phys.* 416:758–762.

Penner, R. 1995. A practical guide to patch clamping. *In* Single-Channel Recording. B. Sakmann and E. Neher, editors. Plenum, New York. 3–30.

Rall, W. 1977. Core conductor theory and cable properties of neurons. *In* The Nervous System; Handbook of Physiology. J. M. Brookhart and V. B. Mountcastle, editors. American Physiological Society, Bethesda, MD. 39–97.

Roberts, W. M. 1987. Sodium channels near end-plates and nuclei of snake skeletal muscle. *J. Physiol. (Lond.).* 388:213–232.

Roberts, W. M., and W. Almers. 1984. An improved loose patch voltage clamp method using concentric pipettes. *Pflugers Arch.* 402:190–196.

Roberts, W. M., and W. Almers. 1992. Patch voltage clamping with low-resistance seals: loose patch clamp. *Methods Enzymol.* 207: 155–176.

Roberts, W. M., R. A. Jacobs, and A. J. Hudspeth. 1990. Colocalization of ion channels involved in frequency selectivity and synaptic transmission at presynaptic active zones of hair cells. *J. Neurosci.* 10:3664–3684.

Sakmann, B., and E. Neher. 1995. Geometric parameters of pipettes and membrane patches. *In* Single-Channel Recording. B. Sakmann and E. Neher, editors. Plenum, New York. 637–650.

Schenkel, S., and F. J. Sigworth. 1991. Patch recordings from the electrocytes of *Electrophorus electricus*. *J. Gen. Physiol.* 97:1013–1041.

Smith, T. G. 1985. Voltage and Patch Clamping with Microelectrodes. American Physiological Society, Bethesda, MD.

Strickholm, A. 1961. Impedance of a small electrically isolated area of the muscle cell surface. *J. Gen. Physiol.* 44:1073–1088.